Interplay of $4f$-$3d$ interactions and spin-induced ferroelectricity in the green phase Gd_2BaCuO_5

Premakumar Yanda,[1] I. V. Golosovsky,[2] I. Mirebeau,[3] N. V. Ter-Oganessian,[4] Juan Rodríguez-Carvajal,[5] and A. Sundaresan[1]

[1]*School of Advanced Materials and Chemistry and Physics of Materials Unit, Jawaharlal Nehru Centre for Advanced Scientific Research, Jakkur P.O. 560064, India*

[2]*National Research Center, Kurchatov Institute, B. P., Konstantinov Petersburg Nuclear Physics Institute, 188300 Gatchina, Russia*

[3]*Université Paris-Saclay, CNRS, CEA, Laboratoire Léon Brillouin, 91191 Gif-sur-Yvette, France*

[4]*Institute of Physics, Southern Federal University, Rostov-on-Don 344090, Russia*

[5]*Institut Laue-Langevin, 71, Avenue des Martyrs, CS 20156, 38042 Grenoble Cedex 9, France*

(Received 19 December 2019; revised manuscript received 31 March 2020; accepted 29 April 2020; published 3 June 2020)

In most of the spin-induced multiferroics, the ferroelectricity is caused by inversion symmetry breaking by complex spin structures of the transition-metal ions. Here, we report the importance of interplay of $4f$-$3d$ magnetic interactions in inducing ferroelectricity in the centrosymmetric (*Pnma*) green phase compound Gd_2BaCuO_5. With decreasing temperature, a long-range incommensurate ordering of both Gd^{3+} and Cu^{2+} spins at $T_N = 11.8$ K occurs with the modulation vector $\mathbf{k} = (0,\ 0,\ g)$ and a lock-in transition to a strongly noncollinear structure with $\mathbf{k}_c = (0,\ 0,\ 1/2)$ at $T_{loc} \sim 6$ K. Both spin structures induce electric polarization consistent with the polar magnetic space groups $Pm1'(\alpha, 0, g)ss$ and P_aca2_1, respectively. Based on the symmetry analysis of magnetoelectric interactions, we suggest that the ferroelectricity in both commensurate and incommensurate phases is driven by a complex interplay of two-spins and single-spin contributions from magnetic ions located in noncentrosymmetric environments. Our study demonstrates that the green phase family of compounds may serve as a playground for studying the multiferroic phenomena, where the interplay of $4f$-$3d$ interactions demonstrates an alternative route to find magnetoelectric materials.

DOI: 10.1103/PhysRevResearch.2.023271

I. INTRODUCTION

Magnetoelectric multiferroics, which allow magnetic-field control of electric polarization and electric-field control of magnetization, have been the subject of great interest in the field of condensed-matter physics due to their fundamental physics and applications in spintronics [1–5]. Along this line, the spin-induced multiferroics, in which certain magnetic orders break inversion symmetry and thus induce electric polarization, attracted much attention because of strong coupling between electric and magnetic orders [2,3]. For example, the well-known rare-earth manganites RMnO$_3$, RMn$_2$O$_5$, Ca$_3$CoMnO$_6$, Ni$_3$V$_2$O$_8$, MnWO$_4$, CoCr$_2$O$_4$, Gd$_{0.5}$Dy$_{0.5}$MnO$_3$, delafossites, and the recently reported aeschynite family of oxides, RFeWO$_6$ (R = Eu, Tb, Dy, and Y), etc. are known to exhibit spin-induced multiferroicity [6–14]. While the layered copper oxides were known for the high-temperature superconductivity, several complex copper oxides such as LiCu$_2$O$_2$, LiCuVO$_4$, CuO, Bi$_2$CuO$_4$, GeCu$_2$O$_4$, and CuFeO$_2$ have been reported to exhibit multiferroic properties [13,15–19]. In all these materials, the microscopic mechanisms responsible for ferroelectricity are the exchange striction, the spin current, or the inverse Dzyaloshinskii-Moriya interaction, and in some cases p-d hybridization [3,7,20].

The green phase compounds R_2BaCuO_5, where R = Sm–Lu and Y, having a centrosymmetric (*Pnma*) crystal structure exhibit a wide range of magnetism and ground-state spin structures due to strong $4f$ and $3d$ interactions [21–25]. In these compounds, the magnetic interactions between Cu^{2+} ions occur through Cu^{2+}–O–R^{3+}–O–Cu^{2+} superexchange path and therefore the magnetic interactions between Cu^{2+}:$3d$ and R^{3+}:$4f$ sublattice moments are important in understanding their magnetic properties. In general, the Cu- and R-sublattice moments in these compounds undergo long-range antiferromagnetic ordering at different temperatures except Gd_2BaCuO_5 where the Cu^{2+} and Gd^{3+} moments order simultaneously around 12 K [25–28]. Previous neutron-diffraction study on Gd_2BaCuO_5 reveals that this compound exhibits incommensurate magnetic structure with a modulation vector $\mathbf{k} = (0,\ 0,\ g)$ below 12 K and undergoes lock-in transition at 5 K to a commensurate magnetic structure with $\boldsymbol{k}_c = (0\ 0\ 1/2)$ [29]. Considering that the magnetic ions are located at the local noncentrosymmetric crystallographic sites [30], we thought that these magnetic structures may induce magnetoelectric properties.

In this paper, we report the observation of ferroelectricity in both commensurate and incommensurate spin states of the compound Gd_2BaCuO_5. Reinvestigation of the previous neutron-diffraction data [29] reveals that the incommensurate ordering corresponds to elliptical cycloidal structure with the

Published by the American Physical Society under the terms of the Creative Commons Attribution 4.0 International license. Further distribution of this work must maintain attribution to the author(s) and the published article's title, journal citation, and DOI.

polar magnetic point group $m1'$, and the low-temperature commensurate phase is strongly noncollinear with the polar magnetic space group P_aca2_1 (point group $mm21'$). We suggest that a complex interplay of two spins and single-spin contributions from ions located in noncentrosymmetric environments are responsible for the multiferroicity.

II. EXPERIMENT

Polycrystalline sample of Gd_2BaCuO_5 was prepared by heating the stoichiometric mixture of high-purity Gd_2O_3 (pre-heated), $BaCO_3$, and CuO at 950 °C in the air as described in Ref. [21]. Magnetization measurements were performed by a superconducting quantum interference device magnetometer (MPMS, Quantum Design). The specific heat (C_p) was measured in the physical property measurement system (PPMS, Quantum Design). To measure the dielectric constant and pyrocurrent (electric polarization), we used 0.46-mm-thickness hardened pellet of polycrystalline Gd_2BaCuO_5 sample covered with an area 25 mm^2 of silver paste, while the temperature and magnetic field control were provided by PPMS. The dielectric constant as a function of temperature under different magnetic fields was recorded using the Agilent E4980A LCR meter. The temperature dependence of pyrocurrent was measured with a Keithley 6517A electrometer and electric polarization was obtained by integrating the pyrocurrent with respect to time. Low-temperature neutron-diffraction data collected at the G61 diffractometer ($\lambda = 4.76$ Å) in the Laboratory Léon Brillouin (Saclay) were used to analyze the crystal and magnetic structure refinements performed by using the FULLPROF program [31].

III. RESULTS AND DISCUSSION

Figure 1(a) depicts the crystal structure of Gd_2BaCuO_5 viewed along the b axis. The refined powder x-ray-diffraction (XRD) pattern and complete structural details are provided in Fig. S1 and Table S1, respectively, in Supplemental Material [32]. In this structure, the oxygen coordination polyhedra of two Gd^{3+} sites differ slightly but the local environments differ significantly. The Gd2 ion is bonded to six nearby copper ions through oxygens, five of the six Gd2–O–Cu bond angles being close to 180°, whereas Gd1 is bonded to only three copper ions at bond angles close to 90°.

The peak of magnetization at 11.8 K at low field (0.01 T) in Fig. 1(b) confirms the long-range antiferromagnetic ordering of Cu^{2+} and Gd^{3+} moments, which is suppressed under applied magnetic fields indicating possible change in the magnetic structure. Upon further cooling, we observe a small anomaly at $T_{loc} \sim 6$ K which is consistent with the lock-in transition [29]. This anomaly shifts to high temperature with applied magnetic fields. The Curie-Weiss fit and field-dependent magnetization are presented in Fig. S2, Supplemental Material [32]. The effective magnetic moment obtained from the fit is $\mu_{eff} = 11.56\,\mu_B$ which is close to the theoretical value of $11.36\,\mu_B$. The negative Curie-Weiss constant is $\theta_{CW} = -4$ K, indicating that dominant interaction is antiferromagnetic. The behavior of $M(H)$ data are consistent with the antiferromagnetic ordering. The long-range order is further confirmed by λ transition at 11.8 K in heat capacity, as

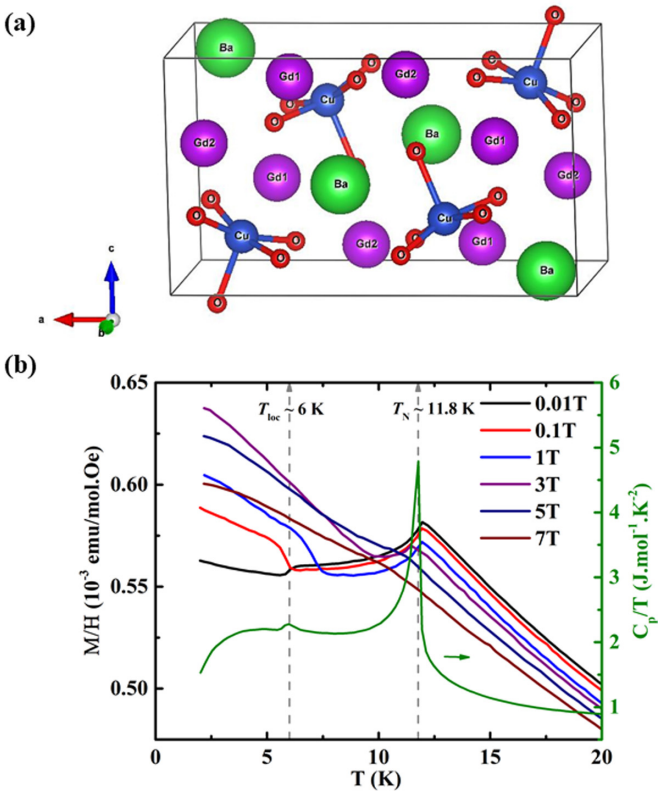

FIG. 1. (a) Schematics of the crystal structure of Gd_2BaCuO_5. (b) Temperature-dependent dc magnetization measured under various magnetic fields in field-cooled sequence (left axis) and specific heat data measured under zero magnetic field.

seen in Fig. 1(b), where a small anomaly at 6 K indicates the lock-in transition.

We observe dielectric anomalies at both the T_N and T_{loc} temperatures under zero magnetic field as shown in Fig. 2(a). The low-temperature anomaly at T_{loc} is suppressed gradually with applied magnetic field and disappears above 0.7 T. On the other hand, the high-temperature anomaly shows a small shift to low temperature and becomes broad. A notable magnetodielectric effect is observed below the magnetic ordering temperature with the value of ~0.05% on an average [32]. To explore whether the dielectric peaks are associated with ferroelectricity, we have recorded temperature-dependent pyroelectric current under different magnetic fields which are shown in Fig. 2(b). Prior to the measurement, we have poled the sample where a magnetic field was applied parallel to the poling electric field. A clear asymmetric peak is seen at the $T_N = 11.8$ K under zero magnetic field, indicating the emergence of spontaneous electric polarization. At T_{loc}, another pyrocurrent peak appears in the same direction, indicating the appearance of a ferroelectric state below T_{loc} with an additional polarization. The corresponding polarization is shown in Fig. 2(c), where the appearance of spontaneous polarization at the onset of magnetic ordering and the enhanced polarization at T_{loc} demonstrate the type-II multiferroic nature of Gd_2BaCuO_5. The value of polarization is 5.5 $\mu C/m^2$ at 2 K under zero magnetic field. We did not observe any significant change when the magnetic field was applied perpendicular to

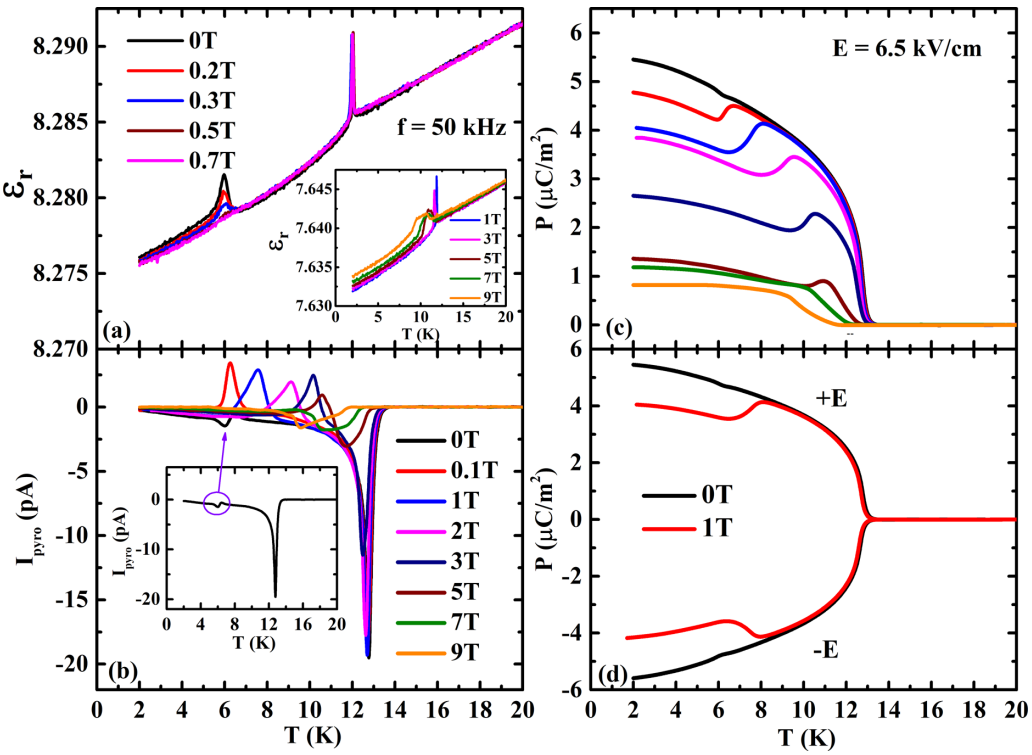

FIG. 2. (a) Dielectric constant (ε_r) as a function of temperature measured under various magnetic fields at the frequency 50 kHz. (b) Pyrocurrent as function of temperature and magnetic field. Inset shows pyrocurrent under zero magnetic field (c) Polarization obtained by integrating the pyrocurrent with respect to time. (d) Polarization measured with positive and negative poling electric fields.

the poling electric field. Interestingly, under applied magnetic fields, the pyrocurrent peaks at $T_{\rm loc}$ are opposite to that at T_N, which is reflected as a dip in polarization and which shifts towards T_N, consistent with the magnetization behavior [Fig. 1(b)]. The switchable nature of electric polarization by changing the direction of poling electric field and observation of dc bias signals (Fig. S4) confirms the intrinsic nature of ferroelectricity as shown in Fig. 2(d) [32]. Hence, our experimental results demonstrate the spin-induced multiferroicity in Gd_2BaCuO_5. It is worth pointing out here that the isostructural compound, Sm_2BaCuO_5 exhibits polarization only under magnetic field, typical of linear magnetoelectric effect [33].

The observation of multiferroicity in Gd_2BaCuO_5 is not consistent with the reported ground-state magnetic structure with magnetic space group $P_S\bar{1}$, which is centrosymmetric and therefore cannot induce ferroelectricity [29]. To unravel the nature of the magnetic ordering, which causes the polarization in Gd_2BaCuO_5, we have reinvestigated the magnetic structure by analyzing low-temperature magnetic powder-diffraction data in more details, using the magnetic space group formalism. Firstly, we have refined the neutron data at 1.3 K by Rietveld method with the magnetic structural model consistent with the wave vector $\mathbf{k}_c = (0,\ 0,\ {}^1/_2)$ and paramagnetic space group $Pnma1'$. The low-temperature magnetic structure obtained from the refinement is commensurate and strongly noncollinear as illustrated in the inset of Fig. 3. The obtained orthorhombic magnetic structure associated with cell doubling along the c axis can be described by magnetic space group P_c2_1ca [Belov-Neronova-Smirnova (BNS) setting that is related to the parent $Pnma1'$ and conserving the same origin **a**,**b**,2**c**;0,0,0]. The transformation to the standard setting P_aca2_1 is performed by **c**,**b**,−**a**;0,1/4,1/8. The refined magnetic moment is 6.73(0.03) μ_B per Gd and 1.02(0.02) μ_B per Cu which are comparable to the theoretical values of 7.0 μ_B per Gd^{3+} and 1 μ_B per Cu^{2+} for fully localized electronic states, respectively. It is important to note that the magnetic space group P_aca2_1 is polar and thus breaks the inversion symmetry of the parent group $Pnma1'$ and induces electric polarization of the form $\mathbf{P}_m = (p_x, 0, 0)$ in the parent setting.

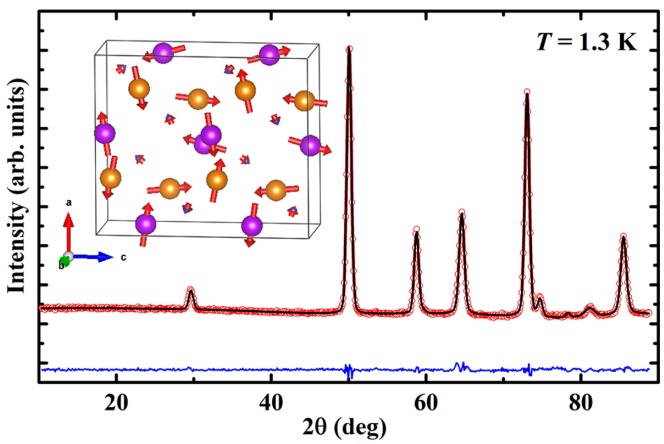

FIG. 3. Refined neutron-diffraction data recorded at 1.3 K. Inset shows the noncollinear commensurate magnetic structure of Gd_2BaCuO_5 at 1.3 K in the magnetic unit cell. (Gd_1, purple; Gd_2, orange; Cu, blue).

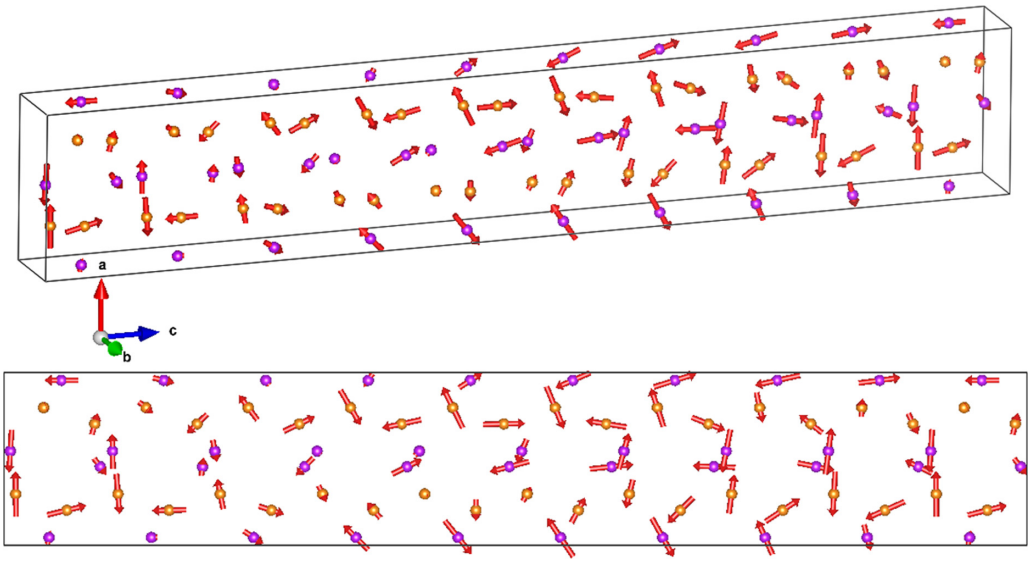

FIG. 4. Magnetic structure of Gd_2BaCuO_5 at 9.8 K viewed along the **b** axis (bottom) and a general orientation (upper part) described in $Pm1'(a, 0, g)ss$. The magnetic structure shown here is constituted by $1 \times 1 \times 10$ unit cells of the paramagnetic structure. The nonmagnetic atoms as well as the Cu atoms have been removed for the sake of clarity. (Gd_1, purple; Gd_2, orange).

On the other hand, for $T_{\rm loc} \leqslant T \leqslant T_N$, the magnetic structure is incommensurate with propagation vector (0, 0, g), with g evolving with decreasing temperature and locking to $g = 1/2$ at 6 K. The symmetry analysis performed with BASIREPS for *Pnma* and with the incommensurate wave vector, using the extended little group, provides four two-dimensional irreducible representations (*irreps*). The main characteristic of all the basis vectors for the position 4*c* is that the corresponding magnetic moments are either along the **b** axis or perpendicular to it. We have used ISODISTORT [34] for determining the possible magnetic modes and the corresponding magnetic superspace groups. The **k** vector corresponds to the point *LD* in the Brillouin zone and, for magnetic modes, the four *irreps* are labeled as: *mLD*1, *mLD*2, *mLD*3, and *mLD*4. We have done systematic tests of all possible solutions using simulated annealing to explore the parameter space for all the maximal magnetic space groups. We found only two possible solutions for the magnetic structure, namely *mLD*2_P(a, 0): $Pnma1'(0, 0, g)0s0s$ and *mLD*2_C(a, b): $Pnm2_11'(0, 0, g)0s0s$. We have mainly worked on the data at 9.8 K because that corresponds to the highest departure from the commensurate $g = 1/2$ value. The amplitude vectors of the magnetic moments are constrained to be in the (**a**, **c**) plane in both cases. Although the overall refinement looks quite good in both cases, it is important to notice that there are few regions in the diffraction pattern where a clear disagreement between the observed and calculated patterns for both models is observed. Going down in symmetry there is only the subgroup $Pm1'(\alpha, 0, g)ss$ as the next candidate which is consistent with the fact that the moments mainly lie in the mirror plane. Indeed, we have found that reliability parameters are better in this case compared with $Pnm2_11'(0, 0, g)0s0s$. The superspace groups of each symmetry mode, refined neutron-diffraction patterns, and complete refinement details are provided in Ref. [32].

The deduced magnetic structure is polar $Pm1'(\alpha, 0, g)ss$ [point group $m1'$, polarization within the (a,c) plane, see below] which is in complete agreement with the observed spontaneous electric polarization appearing at, and below, the Néel temperature. As seen from Fig. 4, the magnetic structure of Gd_2BaCuO_5 is nonconstant moment cycloidal structure because the propagation vector is within the (a, c) plane where moments are lying. The global features of the obtained magnetic structures as a function of the temperature are common to all the refined models: the magnetic structure is basically formed by interpenetrated cycloids with elliptical envelope, so the magnetic moments are not constant. The degree of elliptic shape depends on the particular site. We have to stress that the weak magnetic moment of the Cu makes it difficult to assess the details of this part of the magnetic structure, which may be constrained to have a circular envelope without changing too much the calculated diffraction pattern. For different simulated annealing runs, there are differences in the amplitudes within the zero cell in spite of fixing a polar angle for the first atom; this means that some other magnetic structures seem to fit the experimental data but the difference between them is only a phase between the different sites. It is difficult to compare the magnetic structures looking at the pictures because due to the long period of the modulation in the visualization box we see only a part of the global magnetic structure. We provide the global aspect of the magnetic structure at 9.8 K and its comparison with the commensurate lock-in phase at 1.3 K in Fig. S11, Supplemental Material [32].

We discuss below the theoretical understanding of our experimental results using the symmetry analysis of magnetoelectric interactions. The low-temperature commensurate magnetic structure doubles the crystallographic unit cell along the c axis, whereas the incommensurate magnetic structure possesses the wave vector $\boldsymbol{k}_{\rm inc} = (0, 0, g)$, with g continu-

ously varying from ≈0.4446 at temperature T_N to 1/2 at $T_{\rm loc}$. Thus, the magnetic phase transitions in Gd_2BaCuO_5 are due to the instability at the $\boldsymbol{k}_c$ point of the Brillouin zone, whereas the phase transition at $T_{\rm loc}$ can arguably be considered as a lock-in phase transition. At the $\boldsymbol{k}_c$ point of the Brillouin zone, the paramagnetic space group $Pnma1'$ has two two-dimensional irreducible representations (IR) Z_1 and Z_2. The magnetic representation for each crystallographically different magnetic position (Cu, Gd_1, and Gd_2) splits into $2Z_1 \oplus 4Z_2$ with the x- and z-spin components transforming according to Z_2 and the y components according to Z_1. According to our neutron-diffraction data, in the commensurate phase the spins are confined to the ac plane. The symmetry analysis shows that the magnetic structure can thus be described by the phase state (c, c) of IR Z_2.

Further, we use the magnetic order parameters (OP) (a_1, a_2) and (c_1, c_2), which transform according to Z_2 and may describe the spin components along the a and c axes, respectively, and (b_1, b_2), which transforms according to Z_1 and describes the spin component along the b axis. The OPs (a_1, a_2) and (c_1, c_2) are only 2 of the 12 possible OPs transforming according to Z_2, because this IR enters 12 times into the full magnetic representation of Gd_2BaCuO_5 at $\boldsymbol{k}_c$, whereas (b_1, b_2) is one out of six OPs transforming according to Z_1.

The incommensurate modulation of the high-temperature phase along the z axis is due to the existence of Lifshitz invariants

$$a_1\frac{\partial a_2}{\partial z} - a_2\frac{\partial a_1}{\partial z}, \quad b_1\frac{\partial b_2}{\partial z} - b_2\frac{\partial b_1}{\partial z}, \quad c_1\frac{\partial c_2}{\partial z} - c_2\frac{\partial c_1}{\partial z},$$

which prevent a direct phase transition to the commensurate phase.

The magnetoelectric interactions, constituting the relevant terms of the Landau free-energy polynomial expression, are

$$a_1a_2P_x, \quad c_1c_2P_x, \quad b_1b_2P_x, \tag{1}$$

$$(a_1c_2 + a_2c_1)P_x, \tag{2}$$

$$(a_1c_2 - a_2c_1)P_z, \tag{3}$$

$$(a_1b_1 - a_2b_2)P_y, \qquad (b_1c_1 - b_2c_2)P_y. \tag{4}$$

According to the neutron-diffraction data in both the incommensurate and commensurate phases the spins are confined to the ac plane and the modulated phase is an elliptical cycloidal phase. Therefore, the OP (b_1, b_2) is zero and the magnetic phases are described by a single IR Z_2. Our results indicate that electric polarization appears below T_N and experiences a small anomaly at $T_{\rm loc}$ becoming a more pronounced jump in applied magnetic field. In the modulated phase the magnetoelectric interactions in terms (1) average out to zero and do not contribute to the macroscopic polarization. In turn, depending on the phase shift between the OPs (a_1, a_2) and (c_1, c_2) magnetoelectric interactions in terms (2) and (3) can give rise to macroscopic electric polarization. However, according to neutron diffraction in the elliptical cycloidal phase the spins continuously rotate in the ac plane and the phase shift is such that only term (2) is not zero, whereas term (3) is zero. Therefore, in the modulated phase the electric polarization is directed along the x axis. In the commensurate phase, which is described by the OPs of the form (a, a) and (c, c), additional contribution from the magnetoelectric interactions term (1) appears, which explains the anomaly of polarization at $T_{\rm loc}$. Thus, electric polarization in both magnetically ordered phases has the form $(P_x, 0, 0)$.

In order to understand the microscopic origins of spin-induced electric polarization one can rewrite the magnetoelectric interactions terms (1) and (2) through spins. Since in both the modulated and commensurate phases all the 12 two-component OPs come into play, it appears that magnetoelectric interactions are numerous and are extremely difficult to analyze, however general conclusions can still be made. All three magnetic ions Cu, Gd_1, and Gd_2 are located in local polar environments with local electric dipoles confined to the ac plane. Therefore, the magnetoelectric interactions have single-spin contributions from all spins [30]. However, two-spin contributions to the magnetoelectric interactions are also present and the analysis reveals that they consist of exchange striction terms with $\boldsymbol{P} \sim \boldsymbol{P}_{ij}(\boldsymbol{S}_i \cdot \boldsymbol{S}_j)$ and general contributions from interactions of two canted spins. It has to be noted that the latter are not of the commonly assumed form $\boldsymbol{P} \sim [\boldsymbol{S}_i \times \boldsymbol{S}_j]$ though. Indeed, according to results of neutron diffraction and symmetry analysis the spins are confined to the ac plane whereas electric polarization is directed along the a axis, i.e., lies in the spin rotation plane. The facts that (i) the values of electric polarization are similar in incommensurate and commensurate phases and that (ii) upon approaching the lock-in phase transition the modulated magnetic structure continuously changes to the commensurate state suggest that the microscopic origin of spin-induced electric polarization is the same in both phases. Therefore, we conclude that both single-ion and two-ions interactions with general expressions for electric dipole moment induced by two canted spins [35] as well as exchange striction mechanisms are responsible for magnetoelectric effect in Gd_2BaCuO_5.

The green phase family R_2BaCuO_5 with R = Sm–Lu and Y presents a dozen compounds that according to literature data demonstrate a variety of ground-state magnetic structures depending on the particular R ion owing to the peculiar properties of $4f$-$3d$ magnetic exchange coupling as well as local anisotropic properties of the rare earth. Depending on R, the ground-state magnetic structure possesses different wave vectors, e.g., $\mathbf{k}_c = 0$ (R = Sm [33]), $\mathbf{k}_c = (0,\ 1/2,\ 1/2)$ (R = Y [36]), $\mathbf{k}_c = (0,\ 1/2,\ 0)$ (R = Er, Tm [37]), or $\mathbf{k}_c = (0,\ 0,\ 1/2)$ (R = Gd, this work). The occurrence of linear magnetoelectric effect in Sm_2BaCuO_5 was already shown [33], whereas in this work the multiferroic properties of Gd_2BaCuO_5 are found in accordance with the violation of the Lifshitz criterion for the IRs in $\mathbf{k}_c = (0,\ 0,\ 1/2)$ [30]. According to symmetry analysis, except the U point, all other Brillouin-zone boundary points (i.e., X, Y, Z, T, S, and R) violate the Lifshitz criterion and, thus, the corresponding magnetic structures are candidates for spin-induced electric polarization. Therefore, the variety of magnetic structures in R_2BaCuO_5 suggests the diversity of multiferroic and magnetoelectric properties in the whole

green phase family of compounds. Given this and the fact that solid solutions like $(R', R'')_2BaCuO_5$ (where R' and R'' are different rare earths) should have even more complex magnetic properties, one can conclude that the green phase family may serve as a playground for the studies of multiferroic and magnetoelectric phenomena. The importance of $4f$-$3d$ interactions in the determination of the ground-state magnetic structure suggests that the richness of such phenomena in this class of compounds will arguably overcome that of the orthorhombic rare-earth manganites $RMnO_3$ and manganates RMn_2O_5 including the diversity in electric polarization directions and its magnetic field induced reorientations [6,8]. However, this compound is similar to $RFeO_3$ ($R =$ Gd and Dy) where the $4f$-$3d$ interactions determine the magnetic structure and the ferroelectricity is induced by the exchange striction between the R- and Fe sublattices [38,39]. Our results indicate that external magnetic field has strong influence on electric polarization, T_{loc}, and T_N. However, thorough and substantiated description of the magnetic field effect on magnetic structure and electric polarization requires single-crystal studies and possibly single-crystal neutron diffraction under magnetic field, which will help studying different mutual geometries of magnetic field, electric polarization, and crystal lattice. The polycrystalline nature of the studied samples allows only for a general conclusion that external magnetic field alters the magnetic anisotropy of the system, which is responsible for the lock-in phase transition, and also affects the directions of noncollinear magnetic moments, which are responsible for emergence of electric polarization.

IV. CONCLUSION

In conclusion, we have discovered multiferroicity in Gd_2BaCuO_5 which belongs to well-known green phases. In both the incommensurate and commensurate magnetic phases, spontaneous electric polarization is induced by magnetic ordering. According to the neutron-diffraction data, the polar elliptical cycloidal and the low-temperature commensurate magnetic structures break the inversion symmetry and induce ferroelectricity. We find that Gd_2BaCuO_5 is a type-II multiferroic, in which both single-spin and general two-spin interactions are responsible for the observed multiferroicity. Based on our findings we argue that the whole family of green phase compounds may serve as a rich playground for the studies of multiferroic and magnetoelectric phenomena.

ACKNOWLEDGMENTS

A.S. and P.Y. would like to acknowledge Sheikh Saqr Laboratory (SSL) and International Centre for Materials Science (ICMS) at Jawaharlal Nehru Centre for Advanced Scientific Research (JNCASR) for various experimental facilities. P.Y. acknowledges University Grants Commission (UGC) for Ph.D. Fellowship (Award No. 2121450729). N.V.T. acknowledges financial support by the Russian Foundation for Basic Research Grant No. 18-52-80028 (BRICS STI Framework Programme). I.V.G. acknowledges the financial support from the Russian Foundation for Basic Research (Grant No. 20-02-00109)

[1] D. Khomskii, Physics (College Park, Md.) **2**, 20 (2009).
[2] S.-W. Cheong and M. Mostovoy, Nat. Mater. **6**, 13 (2007).
[3] Y. Tokura, S. Seki, and N. Nagaosa, Rep. Prog. Phys. **77**, 076501 (2014).
[4] R. Ramesh and N. A. Spaldin, Nat. Mater. **6**, 21 (2007).
[5] M. M. Vopson, Crit. Rev. Solid State Mater. Sci. **40**, 223 (2015).
[6] T. Kimura, T. Goto, H. Shintani, K. Ishizaka, T. Arima, and Y. Tokura, Nature (London) **426**, 55 (2003).
[7] I. A. Sergienko, C. Şen, and E. Dagotto, Phys. Rev. Lett. **97**, 227204 (2006).
[8] N. Hur, S. Park, P. A. Sharma, J. S. Ahn, S. Guha, and S.-W. Cheong, Nature (London) **429**, 392 (2004).
[9] Y. J. Choi, H. T. Yi, S. Lee, Q. Huang, V. Kiryukhin, and S.-W. Cheong, Phys. Rev. Lett. **100**, 047601 (2008).
[10] I. Cabrera, M. Kenzelmann, G. Lawes, Y. Chen, W. C. Chen, R. Erwin, T. R. Gentile, J. B. Leão, J. W. Lynn, N. Rogado, R. J. Cava, and C. Broholm, Phys. Rev. Lett. **103**, 087201 (2009).
[11] O. Heyer, N. Hollmann, I. Klassen, S. Jodlauk, L. Bohatý, P. Becker, J. A. Mydosh, T. Lorenz, and D. Khomskii, J. Phys.: Condens. Matter **18**, L471 (2006).
[12] Y. Yamasaki, S. Miyasaka, Y. Kaneko, J. P. He, T. Arima, and Y. Tokura, Phys. Rev. Lett. **96**, 207204 (2006).
[13] T. Kimura, J. C. Lashley, and A. P. Ramirez, Phys. Rev. B **73**, 220401(R) (2006).
[14] S. Ghara, E. Suard, F. Fauth, T. T. Tran, P. S. Halasyamani, A. Iyo, J. Rodríguez-Carvajal, and A. Sundaresan, Phys. Rev. B **95**, 224416 (2017).
[15] S. Park, Y. J. Choi, C. L. Zhang, and S.-W. Cheong, Phys. Rev. Lett. **98**, 057601 (2007).
[16] Y. Naito, K. Sato, Y. Yasui, Y. Kobayashi, Y. Kobayashi, and M. Sato, J. Phys. Soc. Jpn. **76**, 023708 (2007).
[17] T. Kimura, Y. Sekio, H. Nakamura, T. Siegrist, and P. Ramirez, Nat. Mater. **7**, 291 (2008).
[18] L. Zhao, H. Guo, W. Schmidt, K. Nemkovski, M. Mostovoy, and A. C. Komarek, Phys. Rev. B **96**, 054424 (2017).
[19] P. Yanda, S. Ghara, and A. Sundaresan, Solid State Commun. **272**, 53 (2018).
[20] H. Katsura, N. Nagaosa, and A. V. Balatsky, Phys. Rev. Lett. **95**, 057205 (2005).
[21] C. Michel and B. Raveau, J. Solid State Chem. **43**, 73 (1982).
[22] A. Salinas-Sanchez, J. L. Garcia-Muñoz, J. Rodriguez-Carvajal, R. Saez-Puche, and J. L. Martinez, J. Solid State Chem. **100**, 201 (1992).
[23] R. Z. Levitin, B. V Mill, V. V Moshchalkov, N. A. Samarin, V. V Snegirev, and J. Zoubkova, J. Magn. Magn. Mater. **90**, 536 (1990).
[24] A. Salinas-Sánchez, R. Sáez-Puche, and M. A. Alario-Franco, J. Solid State Chem. **89**, 361 (1990).
[25] V. V Moshchalkov, N. A. Samarin, I. O. Grishchenko, B. V Mill, and J. Zoubkova, Solid State Commun. **78**, 879 (1991).

[26] M. Strecker, P. Hettkamp, G. Wortmann, and G. Stewart, J. Magn. Magn. Mater. **177–181**, 1095 (1998).

[27] G. A. Stewart, I. M. McPherson, P. C. M. Gubbens, C. T. Kaiser, P. D. de Reotier, A. Yaouanc, and S. P. Cottrell, J. Alloys Compd. **358**, 7 (2003).

[28] G. F. Goya, R. C. Mercader, L. B. Steren, R. D. Sánchez, M. T. Causa, and M. Tovar, J. Phys.: Condens. Matter **8**, 4529 (1996).

[29] A. K. Ovsyanikov, I. V Golosovsky, I. A. Zobkalo, and I. Mirebeau, J. Magn. Magn. Mater. **353**, 71 (2014).

[30] V. P. Sakhnenko and N. V Ter-Oganessian, J. Phys.: Condens. Matter **24**, 266002 (2012).

[31] J. Rodriguez-Carvajal, in *"Fullprof: A Program for Rietveld Refinement and Pattern Matching Analysis," Abstract of the Satellite Meeting on Powder Diffraction of the XV Congress of the IUCr, Toulouse, France* (1990), p. 127; See also Physica B **192**, 55 (1993). The FULLPROF suite can be freely downloaded from: https://www.ill.eu/sites/fullprof.

[32] See Supplemental Material at http://link.aps.org/supplemental/10.1103/PhysRevResearch.2.023271 for details of XRD, Curie-Weiss fit, magnetization, magnetocapacitance, pyrocurrent, neutron-diffraction data, and their refinement with FULLPROF [31] as well as MCIF files for commensurate and incommensurate structures. These MCIF files can be read with the free web application MVISUALIZE [40,41] that allows one to visualize the structures in three dimensions.

[33] P. Yanda, N. V Ter-Oganessian, and A. Sundaresan, Phys. Rev. B **100**, 104417 (2019).

[34] H. T. Stokes, D. M. Hatch, B. J. Campbell, and D. E. Tanner, J. Appl. Crystallogr. **39**, 607 (2006).

[35] T. A. Kaplan and S. D. Mahanti, Phys. Rev. B **83**, 174432 (2011).

[36] I. V Golosovsky, P. Böni, and P. Fischer, Solid State Commun. **87**, 1035 (1993).

[37] I. V. Golosovsky, V. P. Plakhtii, V. P. Kharchenkov, J. Zoubkova, B. V Mill, M. Bonnet, and E. Roudeau, Fiz. Tve. Tela **34**, 1483 (1992).

[38] Y. Tokunaga, S. Iguchi, T. Arima, and Y. Tokura, Phys. Rev. Lett. **101**, 097205 (2008).

[39] Y. Tokunaga, N. Furukawa, H. Sakai, Y. Taguchi, T. Arima, and Y. Tokura, Nat. Mater. **8**, 558 (2009).

[40] http://webbdcrysta1.ehu.es/magndata/mvisualize.php.

[41] J. M. Perez-Mato, S. V. Gallego, E. S. Tasci, L. Elcoro, G. de la Flor, and M. I. Aroyo, Annu. Rev. Mater. Res. **45**, 217 (2015).